https://doi.org/10.3311/PPme.23707

Periodica Polytechnica Mechanical Engineering, 68(1), pp. 63–69, 2024

Investigation of the Bending Properties of *Ex situ* Functional Metal Foams

Gábor Pados[1,2*], Alexandra Kemény[1,2], Dóra Károly[1,2], Imre Norbert Orbulov[1,2]

[1] Department of Materials Science and Engineering, Faculty of Mechanical Engineering, Budapest University of Technology and Economics, Műegyetem rkp. 3., H-1111 Budapest, Hungary
[2] MTA-BME Lendület "Momentum" High-performance Composite Metal Foams Research Group, Műegyetem rkp. 3., H-1111 Budapest, Hungary
[*] Corresponding author, e-mail: padosgabor@edu.bme.hu

Received: 25 October 2023, Accepted: 01 December 2023, Published online: 25 January 2024

Abstract

In each industry, compromises have to be made when choosing materials. Lower-density materials have a significant advantage in the automotive sector, especially due to rising fuel prices, since weight reduction can lower overall fuel consumption. The advantageous properties of metal foams, such as low density, high specific strength, and excellent energy absorption, should be researched and exploited in as many areas and ways as possible. This research aims to perform and evaluate the bending tests of *ex situ* functional metal foams: aluminum alloy matrix (AlSi7Mg) was used, which was filled with Ø2.5–3.0 mm lightweight expanded clay aggregate particles and surrounded by thin-walled aluminum tubes (AlMgSi0.5) with a wall thickness of 2 mm and an outer diameter of Ø32 mm. Empty tubes, foam-filled tubes (with and without structural epoxy adhesive) and metal matrix syntactic foams were compared based on their flexural strength and energy absorption capacity. Quasi-static three-point bend tests were carried out up to 25 mm deflection. The foam-filled tubes with epoxy adhesive showed an average of 6% increase in flexural strength compared to the foam-filled tubes without adhesive and a 145% increase compared to the metal matrix syntactic foams.

Keywords

syntactic metal foams, foam-filled tubes, bending properties

1 Introduction

Composite metal foams are hybrid structures with several important advantages, such as high specific strength, low density, and excellent mechanical energy absorption, while providing thermal and chemical stability [1–3].

Metal matrix syntactic foams (MMSFs) are rarely produced as functional, structural materials; they are primarily researched as bare foams and space-filling parts. It is not very complicated or expensive to manufacture MMSFs, but extreme care must be taken to set the parameters correctly and to monitor the correctness of the procedure. Usually, there is a large difference between the melting points of the mold used and the matrix material, so there should not be any significant problems during casting; however, proper pressure and pre-heating must be applied. Metal foams are generally characterized by their energy-absorbing properties; currently, compression testing is the only internationally standard measurement [4–7].

Nevertheless, metal foams can be placed or adhesively bonded between dense sheets [8] or inside a tube (*ex situ* production). It is also possible that foams are foamed inside or infiltrated into a tube in one step (*in situ* production). Foam-filled tubes (FFTs) are structural materials that can achieve high energy absorption even with low additional weight [9–16].

Most articles on metal FFTs are on the axial compressive properties of closed-cell aluminum foam-filled aluminum [17, 18] or steel tubes [19–21]. Furthermore, some deal with radial compression [22, 23], and a few with three-point bending; the latter articles are detailed below. In Duarte et al.'s [9] research, cylindrical samples of aluminum alloy closed-cell metal foams were produced using the powder metallurgy method and placed into thin-walled tubes made of aluminum alloy AA 6060 T66 (AlMgSi0.5). In the case of the FFTs, the crack started in the foam and then spread onto the outer tube. The FFTs had the highest

Cite this article as: Pados, G., Kemény, A., Károly, D., Orbulov, I. N. "Investigation of the Bending Properties of *Ex situ* Functional Metal Foams", Periodica Polytechnica Mechanical Engineering, 68(1), pp. 63–69, 2024. https://doi.org/10.3311/PPme.23707

load capacity but fractured at much lower deformation, which occurred suddenly compared to the empty tube. In addition, it was also found that by combining two structures, the energy absorption capacity can be increased without a significant increase in weight.

Shojaeifard et al. [16] examined elliptical, circular and square tubes of the same aluminum alloy (6063-T3) with different wall thicknesses (1.5 mm and 2.0 mm). The energy absorption of aluminum foam-filled square and circular tubes was approximately 18% and 38% higher, respectively, compared to empty tubes.

In Zhang et al.'s [24] research, closed-cell aluminum alloy foams were placed in 6063 T5 aluminum alloy tubes. The external dimensions of the tubes were 15 × 6 × 360 mm, and the wall thickness of the tubes was 0.8 mm. The ready-made aluminum alloy foam was placed into the tube without adhesive. The research showed that the strength of the foam core, the wall thickness of the tube and the diameter of the supports during the bend tests significantly affect the structural response of the FFTs. The axial stretching induced by large deflection plays an important role in the post-yield regime of the foam-filled rectangular tube.

In a recent research, Chilla et al. [25] examined 316L stainless steel tubes filled with open-cell aluminum foam. *Ex situ* FFTs were produced by inserting the foam into uncoated tubes, and *in situ* FFTs were fabricated by foaming an Al-6Si-4Cu-2Mg alloy precursor inside uncoated and copper-coated tubes. This latter method was proven to be a successful procedure, as after the aluminum was foamed, the continuous copper coating disappeared, and the reaction product was formed at the interface between the foam and the tube, which contained aluminum, copper, tin, and iron. The specimens made with copper-coated tubes established an excellent bond between the foam and the tube, and no air gap was observed between them, even after the compressive test was completed. The bond enabled the foam-tube interaction during the entire deformation process, which resulted in the foam being trapped between the folds created during compaction; therefore, the highest compressive strength and specific energy absorption (10% increase) could be measured for these test specimens. The difference could also be observed in the bending test results, but with no difference in the failure mode and a lower improvement in the properties. An important conclusion of the study is that if no additional layer is used to promote bonding, the *in situ* FFTs showed only slightly improved properties compared to the foam cores placed tightly inside the tube.

Garai et al. [18] produced *ex situ* circular closed-cell FFTs with three different insertion methods. They found that the adhesive-bonded FFTs had the highest strength and energy absorption values during three-point bending, the foams that were inserted with mechanical pressing into the tubes resulted in lower strength, and the FFTs that were joined by heat dilatation had the lowest values. The authors concluded that *ex situ* foam-filled elements can be used in the safety systems of automobiles.

Zhang et al. [14] investigated the bending properties of fly ash cenosphere-filled MMSF-cores in stainless steel tubes with 50% and 100% foam fillings. It was concluded that the foam-filled fraction dominates the failure mode; however, combined with finite element analysis, they stated that the bending properties of FFTs were more sensitive to the tube wall-thickness than to the foam-filled fraction.

Taherishargh et al. [26] produced *in situ* AlSi7Mg FFTs with expanded perlite-filled MMSF cores and stainless steel tubes. The overall properties of the FFTs with 0.9 mm wall-thickness were superior to the 1.2 mm walled FFTs. The authors found a reaction zone between the tube and the matrix. Additionally, the tensile strength was estimated from the flexural strength.

Compared to previous research articles, MMSFs were placed and adhesive bonded into empty tubes in this paper. The samples were loaded with three-point bending, where both compression and tension occur through the cross-section of the FFTs.

2 Materials and methods

2.1 Materials

During the research, aluminum alloy matrix AlSi7Mg MMSFs were placed in AlMgSi0.5 aluminum alloy tubes. Lightweight expanded clay aggregate particles (LECAPs) sold by Liapor GmbH & Co. KG were used as fillers, with the chemical composition of ~60 wt% SiO_2, ~17 wt% Al_2O_3, ~14 wt% Fe_2O_3 and other oxides (CaO, MgO, Na_2O, K_2O). The particles were sieved into the size range of Ø2.5–3.0 mm. The properties of the fillers were measured in a previous study [27].

2.2 Manufacturing

For the bend tests, MMSF cylinders were made. The manufacturing process began with coating the inside of the steel crucibles (60 × 60 mm cross-section, 240 mm high square-based column) with N-77 graphite spray (DUE-CI ELECTRONIC s.n.c., Avesa, Italy). The drilled gas outlet on the side was then filled with an alumina quilt to prevent

the melt from flowing through. The stability of the quilt was promoted by reducing the cross-section of the outlet. Then the crucible was filled with ~300 ml of LECAPs, and a stainless-steel net was placed on top of the particles, which prevented the LECAPs from floating up in the aluminum melt. The steel crucibles were then preheated in a Lindberg/Blue M box furnace (Thermo Fisher Scientific Inc., Waltham, MA, USA) at 600 °C and kept there for at least 30 minutes so that the crucible and all the LECAPs reached the set temperature. Meanwhile, the AlSi7Mg blocks were heated to a glowing red state (~850 °C) in an IND IF-10 induction melting furnace (Inductor. Ltd., Diósd, Hungary). Once this state was reached, the machine was turned off, and the melt temperature was measured during cooling with a Maxthermo MD-3003K digital thermometer (Maximum Electronic Co Ltd., New Taipei City, Taiwan). The melt was poured into the preheated steel crucible filled with LECAPs at a temperature between 750 °C–800 °C. The required pressure for infiltration was applied through an insulated pipe, which was connected to a high-pressure argon bottle through a reducer, and a pressure of 500 kPa was applied to press the melt. Schematic images of the infiltration installation can be found in previous articles by the authors [13, 28].

After the now foam-filled crucible was cooled, the MMSF block was removed, and samples were machined into 160 mm long, ~Ø26 mm diameter cylinders for the three-point bending tests (see Table 1). To fabricate the functional MMSFs as FFTs, AlMgSi0.5 tubes with Ø32 mm outer diameter and 2 mm wall thickness were cut into 160 mm long pieces.

Before the fabrications of the FFTs, a heat-treatment process, namely precipitation hardening (shown in Fig. 1), was used to increase the strength of the used aluminum

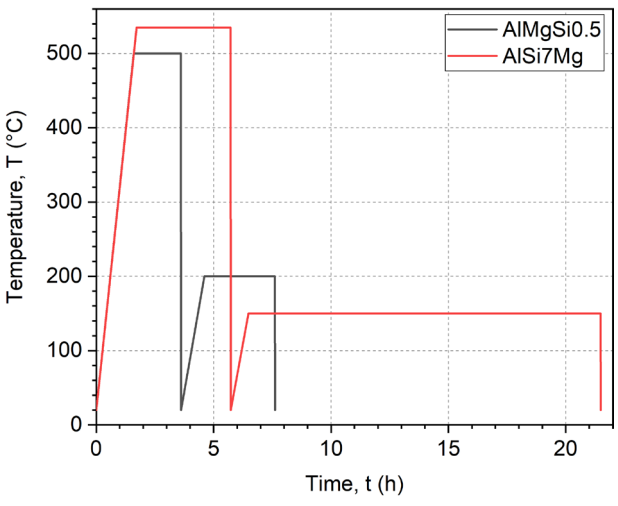

Fig. 1 Heat-treatment cycles of the applied materials

alloys. Precipitation hardening leads to the formation of fine precipitates within the aluminum matrix; hence, these particles obstruct the movement of dislocations in the crystal structure, thereby increasing the overall strength, hardness and wear resistance of the material, while the initial ductility is also preserved [13].

The density data of the fabricated syntactic metal foams is also detailed in Table 1. Density plays a pivotal role in metal foams and foam-filled structures by having a pronounced influence on various advantageous structural properties, including energy absorption capacity and the extent of weight reduction. As shown in the fourth column of Table 1, the recorded values for foam density have an average of 1.48 ± 0.05 g/cm^3, nearly half compared to the density of the utilized aluminum alloy matrix and tube. The third column of Table 1 shows the density values of the manufactured specimens, depending on their type (whether adhesive bonded or just placed). In each case, there is a noteworthy reduction in weight compared to the initial density of aluminum.

The heat-treated MMSFs were inserted or adhesive bonded into heat-treated tubes with 3M™ Scotch-Weld™ DP410 epoxy adhesive (3M Co., Saint Paul, MN, USA) (Fig. 2).

2.3 Bend tests

During the examination, a total of 12 samples were investigated: MMSFs placed in tubes (f-MMSFs), MMSFs adhesive bonded in tubes (f-EMMSFs), empty tubes (ET) and MMSFs (without tubes). The bend tests were performed according to ISO 7438:2020 [29], on an MTS810 hydraulic universal material testing device equipped with

Table 1 The actual densities and diameters of the specimens

Sample	Specimen	Density (g/cm^3)	Density of the foam (g/cm^3)	Diameter of the foam (mm)
f-MMSFs	f-MMSF_1	2.10	1.45	26.1
	f-MMSF_2	2.04	1.46	25.1
	f-MMSF_3	2.09	1.49	26.1
	f-MMSF_4	1.99	1.49	25.1
f-EMMSFs	f-EMMSF_1	2.16	1.45	26.0
	f-EMMSF_2	1.94	1.43	24.1
	f-EMMSF_3	2.12	1.51	26.1
	f-EMMSF_4	2.03	1.50	25.1
MMSFs	MMSF_1	1.42	1.42	27.6
	MMSF_1	1.60	1.60	27.7
ETs	ET_1	2.67	-	-
	ET_2	2.70	-	-

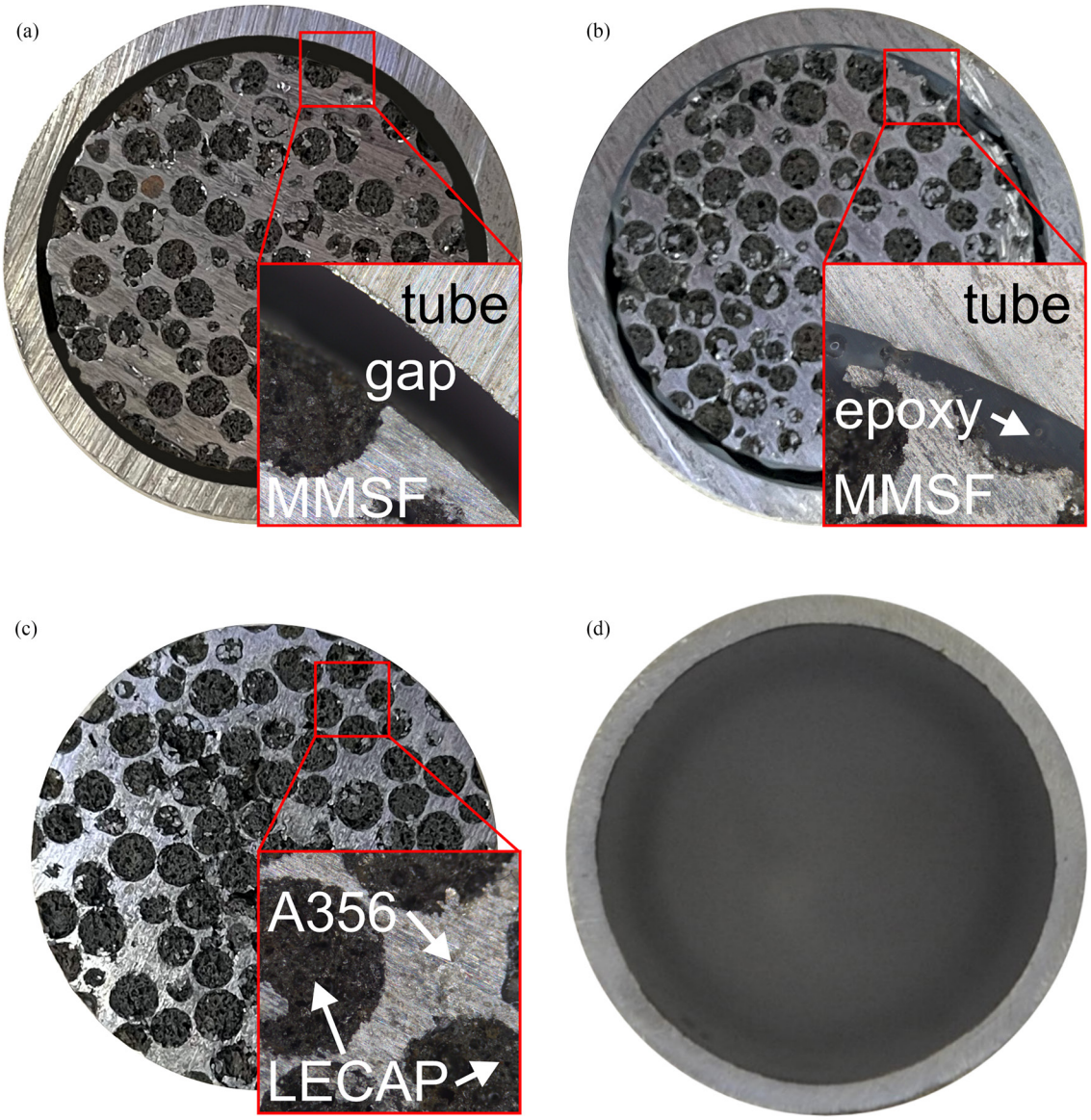

Fig. 2 The four types of samples: (a) MMSFs placed in tubes (f-MMSFs), (b) MMSFs adhesively bonded into tubes (f-EMMSFs), (c) MMSFs and (d) empty tubes (ET)

a 250 kN load cell. The length between the supports was 140 mm, and the diameter of the supports and the loading roller was Ø14 mm. The crosshead speed was set to 5 mm/min. The tests were recorded with a mounted camera for monitoring the deformation process (Fig. 3).

The absorbed energy, maximum force, and flexural strength were determined during the evaluation. The latter was calculated by dividing the maximum bending moment (which can be derived from the force) by the effective section modulus (calculated as the section modulus of the whole section, neglecting the pores) of the samples. The absorbed energy was calculated at different deflections, with 5 mm steps (δ = 5 mm–25 mm).

3 Results and discussion

During the bend tests, a higher amount of absorbed energy and strength can be observed for the functional MMSFs compared to the bare MMSFs. Inside the tubes, the fracture of the non-adhesive bonded f-MMSFs showed a sudden force drop on the curve (Fig. 4 (a)), but the energy absorption did not stop due to the deformation capacity surplus of the outer tube. After the MMSF core fractured, the tube did not crack on its tensile side but started to push the MMSF out on the free sides. In the case of the adhesive-bonded f-EMMSFs, the failure and their curves were similar to that of the f-MMSFs. In the case of the f-EMMSF with the smallest diameter MMSF core,

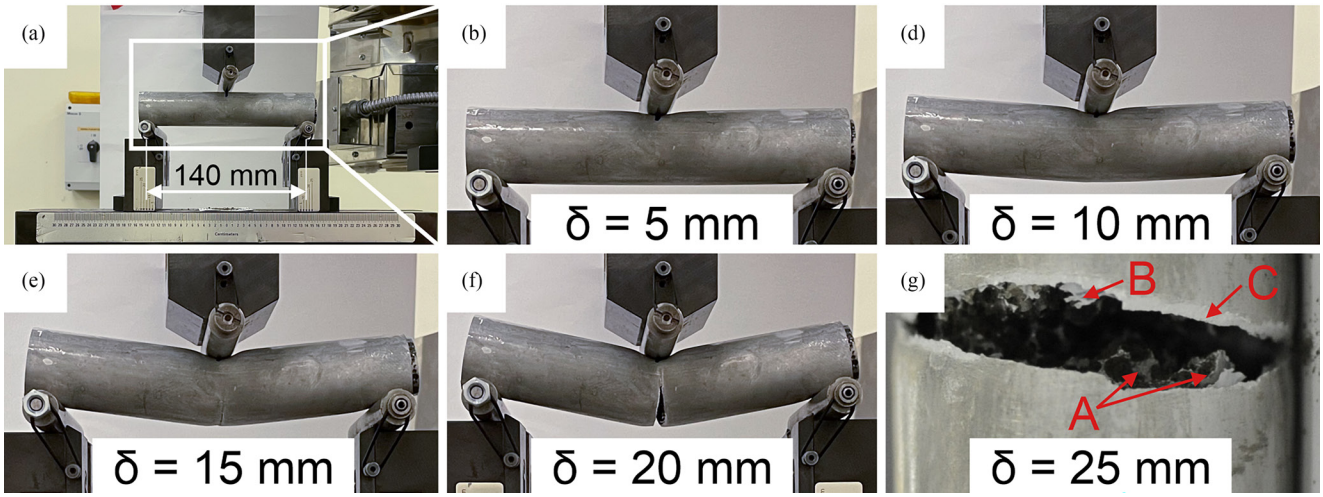

Fig. 3 Captures of the bend test of an f-EMMSF. (a) experimental setup without displacement, (b) 5 mm, (c) 10 mm, (d) 15 mm and (e) 20 mm deformation of the f-EMMSF structure during bending, and (f) a close-up of the cracked side, where the A: brittle fracture of the MMSF core, B: the torn epoxy adhesive and C: the plastic deformation of the tube is visible

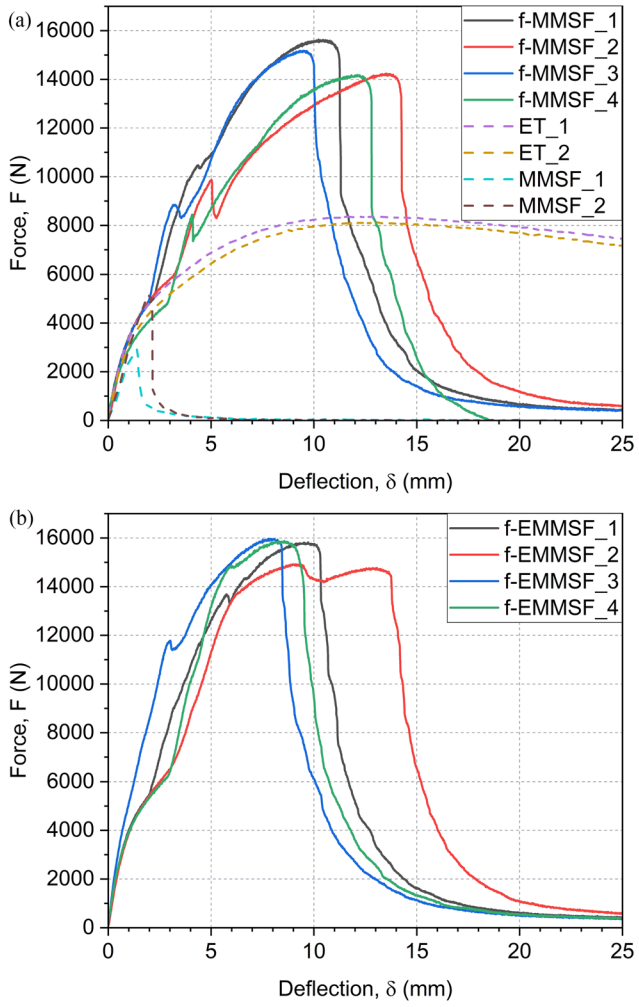

Fig. 4 Bending results of (a) f-MMSFs, ETs and MMSFs and (b) f-EMMSFs

the failure occurred at a larger deflection (Fig. 4 (b), red curve), as the ductility was preserved up to a larger deformation, resulting in higher absorbed energy compared to the other functional MMSFs with or without adhesive. Therefore, the gap between the tube and the MMSF core influences the energy absorption capacity.

The difference between the f-MMSFs and f-EMMSFs is due to the gap between the tube and the MMSF core, which has been partially filled in the adhesive-bonded case. The bare MMSF cannot absorb a high amount of energy, they have a low flexural strength and have a brittle fracture at a very low deflection (~2 mm), but when it was adhesively bonded to a tube, the energy absorption increased by 2300%, and the flexural strength by 137% in average.

High energy absorption was observed when the ETs were bent, but the maximum flexural strength was 45% smaller on average than that of the functional MMSFs. However, compared to the bending energy absorption of the empty tubes, the structures that contained MMSFs had brittle fractures at lower deflections, resulting in an overall smaller energy absorption at the end of the test (Table 2, $W_{25\ mm}$).

Table 2 Average energy absorbed by different specimen types at different deflections, the maximum force value, and the flexural strength

Sample	f-MMSF	f-EMMSF	MMSF	ET
$W_{5\ mm}$ (J)	29 ± 2	36 ± 3	6 ± 1	23 ± 1
$W_{10\ mm}$ (J)	91 ± 5	107 ± 2	6 ± 1	61 ± 1
$W_{15\ mm}$ (J)	136 ± 3	139 ± 5	6 ± 1	102 ± 2
$W_{20\ mm}$ (J)	143 ± 7	145 ± 12	6 ± 1	142 ± 2
$W_{25\ mm}$ (J)	144 ± 8	148 ± 13	6 ± 1	179 ± 3
F_{max} (N)	14807 ± 359	15647 ± 243	8264 ± 90	4064 ± 90
σ_b (MPa)	159 ± 4	169 ± 3	69 ± 14	90 ± 1

4 Conclusions

Due to the brittleness of metal foams, they do not resist bending stress. With the use of outer tubes, the applicability of foam structures under bending can be enhanced. Based on the results, there was no significant difference between the failure of metal matrix syntactic foams (MMSFs) placed in tubes (f-MMSFs) and MMSFs adhesive bonded in tubes (f-EMMSFs) during three-point bending; however, the presence of the epoxy adhesive had a slight positive effect on the ductility so that a 3% greater energy absorption and 6% higher flexural strength can be achieved during bending. Changing the gap size between the tube and the MMSF core and using various adhesive amounts offer promising opportunities for further research on the topic.

Acknowledgements

Project no. TKP-6-6/PALY-2021 has been implemented with the support provided by the Ministry of Culture and Innovation of Hungary from the National Research, Development and Innovation Fund, financed under the TKP2021-NVA funding scheme. G. Pados was supported by the ÚNKP-23-2-I-BME-180 New National Excellence Program of the Ministry for Culture and Innovation from the source of the National Research, Development and Innovation Fund. This work was partially supported by the National Research, Development and Innovation Office (NKFIH), under grant agreement OTKA-FK_21 138505.

References

[1] Gupta, N., Woldesenbet, E., Mensah, P. "Compression properties of syntactic foams: effect of cenosphere radius ratio and specimen aspect ratio", Composites Part A: Applied Science and Manufacturing, 35(1), pp. 103–111, 2004. https://doi.org/10.1016/j.compositesa.2003.08.001

[2] Kemény, A., Leveles, B., Károly, D. "Functional aluminium matrix syntactic foams filled with lightweight expanded clay aggregate particles", Materials Today: Proceedings, 45, pp. 4229–4232, 2021. https://doi.org/10.1016/j.matpr.2020.12.164

[3] Orbulov, I. N., Szlancsik, A. "On the Mechanical Properties of Aluminum Matrix Syntactic Foams", Advanced Engineering Materials, 20(5), 1700980, 2018. https://doi.org/10.1002/adem.201700980

[4] Su, M., Wang, H., Hao, H., Fiedler, T. "Compressive properties of expanded glass and alumina hollow spheres hybrid reinforced aluminum matrix syntactic foams", Journal of Alloys and Compounds, 821, 153233, 2020. https://doi.org/10.1016/j.jallcom.2019.153233

[5] Su, M., Li, J., Li, M., Hao, H. "Microstructure and mechanical properties of bimodal syntactic foams with different size combination and volume fraction of alumina hollow spheres", Materials Science and Engineering: A, 824, 141798, 2021. https://doi.org/10.1016/j.msea.2021.141798

[6] Jenei, P., Kádár, C., Szabó, Á., Hung, S.-M., Kuo, C.-J., Choe, H., Gubicza, J. "Mechanical behavior of freeze-cast Ti foams with varied porosity", Materials Science and Engineering: A, 855, 143911, 2022. https://doi.org/10.1016/j.msea.2022.143911

[7] Kádár, C., Kubelka, P., Szlancsik, A. "On the compressive properties of aluminum and magnesium syntactic foams: Experiment and simulation", Materials Today: Communicatons, 35, 106060, 2023. https://doi.org/10.1016/j.mtcomm.2023.106060

[8] Kaffash Mirzarahimi, M., Khodarahmi, H., Ziashamami, M., Hosseini, R. "Numerical and Experimental Study of the Use of Mineral Pumice in the Core of the Sandwich Panel to Absorb the Shock Wave", Periodica Polytechnica Mechanical Engineering, 67(1), pp. 19–29, 2023. https://doi.org/10.3311/PPme.19341

[9] Duarte, I., Vesenjak, M., Krstulović-Opara, L. "Dynamic and quasi-static bending behaviour of thin-walled aluminium tubes filled with aluminium foam", Composite Structures, 109, pp. 48–56, 2014. https://doi.org/10.1016/j.compstruct.2013.10.040

[10] Duarte, I., Vesenjak, M., Krstulović-Opara, L., Anžel, I., Ferreira, J. M. F. "Manufacturing and bending behaviour of *in situ* foam-filled aluminium alloy tubes", Materials & Design, 66, pp. 532–544, 2015. https://doi.org/10.1016/j.matdes.2014.04.082

[11] Vesenjak, M., Duarte, I., Baumeister, J., Göhler, H., Krstulović-Opara, L., Ren, Z. "Bending performance evaluation of aluminium alloy tubes filled with different cellular metal cores", Composite Structures, 234, 111748, 2020. https://doi.org/10.1016/j.compstruct.2019.111748

[12] Baumgärtner, F., Duarte, I., Banhart, J. "Industrialization of Powder Compact Foaming Process", Advanced Engineering Materials, 2(4), pp. 168–174, 2000. https://doi.org/10.1002/(sici)1527-2648(200004)2:4<168::aid-adem168>3.0.co;2-o

[13] Kemény, A., Leveles, B., Kincses, D. B., Károly, D. "Manufacturing and Investigation of In Situ and Ex Situ Produced Aluminum Matrix Foam-Filled Tubes", Advanced Engineering Materials, 24(1), 2100365, 2022. https://doi.org/10.1002/adem.202100365

[14] Zhang, B., Zhang, J., Wang, L., Jiang, Y., Wang, W., Wu, G. "Bending behavior of cenosphere aluminum matrix syntactic foam-filled circular tubes", Engineering Structures, 243, 112650, 2021. https://doi.org/10.1016/j.engstruct.2021.112650

[15] Reyes, A., Hopperstad, O. S., Hanssen, A. G., Langseth, M. "Modeling of material failure in foam-based components", International Journal of Impact Engineering, 30(7), pp. 805–834, 2004. https://doi.org/10.1016/j.ijimpeng.2004.03.008

[16] Shojaeifard, M. H., Zarei, H. R., Talebitooti, R., Mehdikhanlo, M. "Bending behavior of empty and foam-filled aluminum tubes with different cross-sections", Acta Mechanica Solida Sinica, 25(6), pp. 616–626, 2012. https://doi.org/10.1016/S0894-9166(12)60057-3

[17] Kavi, H., Toksoy, A. K., Guden, M. "Predicting energy absorption in a foam-filled thin-walled aluminum tube based on experimentally determined strengthening coefficient", Materials & Design, 27(4), pp. 263–269, 2006. https://doi.org/10.1016/j.matdes.2004.10.024

[18] Garai, F., Béres, G., Weltsch, Z. "Development of tubes filled with aluminium foams for lightweight vehicle manufacturing", Materials Science and Engineering: A, 790, 139743, 2020. https://doi.org/10.1016/j.msea.2020.139743

[19] Rajak, D. K., Mahajan, N. N., Linul, E. "Crashworthiness performance and microstructural characteristics of foam-filled thin-walled tubes under diverse strain rate", Journal of Alloys and Compounds, 775, pp. 675–689, 2019. https://doi.org/10.1016/j.jallcom.2018.10.160

[20] Linul, E., Movahedi, N., Marsavina, L. "The temperature effect on the axial quasi-static compressive behavior of *ex-situ* aluminum foam-filled tubes", Composite Structures, 180, pp. 709–722, 2017. https://doi.org/10.1016/j.compstruct.2017.08.034

[21] Movahedi, N., Linul, E. "Quasi-static compressive behavior of the ex-situ aluminum-alloy foam-filled tubes under elevated temperature conditions", Materials Letters, 206, pp. 182–184, 2017. https://doi.org/10.1016/j.matlet.2017.07.018

[22] Movahedi, N., Linul, E. "Radial crushing response of *ex-situ* foam-filled tubes at elevated temperatures", Composite Structures, 277, 114634, 2021. https://doi.org/10.1016/j.compstruct.2021.114634

[23] Wang, L., Zhang, B., Zhang, J., Jiang, Y., Wang, W., Wu, G. "Deformation and energy absorption properties of cenosphere-aluminum syntactic foam-filled tubes under axial compression", Thin-Walled Structures, 160, 107364, 2021. https://doi.org/10.1016/j.tws.2020.107364

[24] Zhang, J., Qin, Q., Yang, Y., Yu, X., Chen, S., Wang, T. J. "Large-Deflection Bending of Clamped Metal Foam-Filled Rectangular Tubes", International Journal of Applied Mechanics, 9(3), 1750043, 2017. https://doi.org/10.1142/S1758825117500430

[25] Chilla, V., Mondal, D. P., Ram, G. D. J., Mukherjee, M. "Processing of in-situ aluminium foam-filled stainless steel tube with foam-tube bonding for enhanced crashworthiness", Journal of Manufacturing Process, 82, pp. 488–500, 2022. https://doi.org/10.1016/j.jmapro.2022.08.020

[26] Taherishargh, M., Vesenjak, M., Belova, I. V., Krstulović-Opara, L., Murch, G. E., Fiedler, T. "*In situ* manufacturing and mechanical properties of syntactic foam filled tubes", Materials & Design, 99, pp. 356–368, 2016. https://doi.org/10.1016/j.matdes.2016.03.077

[27] Szlancsik, A., Katona, B., Kemény, A., Károly, D. "On the Filler Materials of Metal Matrix Syntactic Foams", Materials, 12(12), 2023, 2019. https://doi.org/10.3390/ma12122023

[28] Orbulov, I. N., Szlancsik, A., Kemény, A., Kincses, D. "Compressive mechanical properties of low-cost, aluminium matrix syntactic foams", Composite Part A: Applied Science and Manufacturing, 135, 105923, 2020. https://doi.org/10.1016/j.compositesa.2020.105923

[29] International Organization for Standardization "ISO 7438:2020 Metallic materials: Bend test", ISO, Geneva, Switzerland, 2020.